Journal of Membrane Science Letters 3 (2023) 100055

Contents lists available at ScienceDirect

Journal of Membrane Science Letters

journal homepage: www.elsevier.com/locate/memlet

Effect of surfactant structure on MPD diffusion for interfacial polymerization

Shahriar Habib, Bryn E. Larson, Steven T. Weinman*

Department of Chemical and Biological Engineering, The University of Alabama, Tuscaloosa, AL 35487, USA

ARTICLE INFO

Keywords:
Thin-film composite membrane
Interfacial tension
Fully aromatic polyamide
Surfactants
Reverse osmosis

ABSTRACT

Polyamide membranes made with surfactant-assisted interfacial polymerization (IP) have demonstrated the potential for excellent membrane performance. The presence of surfactants accelerates amine diffusion into the organic phase causing a more complete IP reaction. Even though surfactant-assisted IP has been used in polyamide membranes, the structure-property relationship of the surfactants on amine transport into the organic phase has not been explored in a systematic manner. In this work, MPD diffusion from a membrane support into *n*-dodecane in the presence of seven different surfactants, which were anionic, cationic, and non-ionic, was evaluated. When the surfactants were used at different concentrations, the MPD concentration was increased in the presence of anionic (48–80%), cationic (32–75%) and non-ionic (26%) surfactants. The MPD concentration was increased in the presence of anionic (by 48–72%), cationic (by 32–75%), and non-ionic surfactants (by 26%) at 15–60 s contact time. For further understanding, the interfacial tension in *n*-dodecane for the surfactants was measured, however, it did not correlate with our data. This study provides a better understanding of MPD diffusion in the presence of different types of surfactants during RO membrane synthesis, which will help us to engineer membranes with better permeability and selectivity.

1. Introduction

For the past four decades, science has advanced polyamide reverse osmosis (RO) membranes to remove small ions and contaminants in water very effectively. During the synthesis of RO membranes, the interfacial polymerization (IP) reaction between the amine and acyl chloride monomers produces a polyamide separation layer on an ultrafiltration support membrane (Habib and Weinman, 2021). Because the monomers used for IP are highly reactive, the reaction is challenging to control but can be affected by monomers' diffusion behavior (Wittbecker and Morgan, 1959). During IP, m-phenylenediamine (MPD) initially diffuses into the organic layer and reacts instantaneously with TMC to form an incipient layer of polyamide which densifies and reduces MPD diffusion towards the aqueous/organic interface and limits polyamide growth (Grzebyk et al., 2022), resulting in polyamide separation layers with multiscale heterogeneity and non-uniform pore or free volume hole size distributions (Zhang et al., 2020). Thus, the IP reaction determines membrane selectivity primarily by diffusion and reaction. Therefore, it is important but challenging to develop an effective method for controlling the diffusion of MPD monomers in polyamide RO membranes to improve their selectivity.

An innovative method of membrane preparation involves mixing additives with aqueous or organic solutions to regulate the formation and stacking of PA molecules (Liu et al., 2020, 2019; Zhang et al., 2019). The chemical and physical structure of the polyamide layer can be designed by using additives, developing new monomers, optimizing the IP process, and/or post-modification methods (Habib and Weinman, 2021; Habib and Weinman, 2022; Lu and Elimelech, 2021; Hu et al., 2023; Farahbakhsh et al., 2021). In previous studies, surfactants incorporated into the aqueous phase of the IP reaction led to high-flux and higher rejection RO and nanofiltration (NF) membranes (Liu et al., 2020; Liang et al., 2020; Xiang et al., 2013, 2014; Sarkar et al., 2021; Li et al., 2022; Bai et al., 2022; Jiang et al., 2019; Fang et al., 2013; Ang et al., 2020; Zhang et al., 2021; Park et al., 2022; Han et al., 2022; Kong et al., 2011; Duan et al., 2010; Gan et al., 2023). Liang et al. used anionic, cationic, and zwitterionic surfactants during the synthesis of semi-aromatic polyamide NF membranes and illustrated with molecular dynamics simulations that inclusion of surfactants led to the formation of dynamic interfacial networks (Liang et al., 2020). Through this dynamic network, amine monomers accumulate at the interface while also diffusing rapidly into the organic phase and being evenly distributed since Gibbs free energy is reduced. The addition of a surfactant during IP produced a polyamide separation layer with more uniform pores compared to conventional IP, resulting in membranes with better ion rejection (Liang et al., 2020). Zhang et al. examined the structure of the polyamide separation layers using sulfate surfactants with differ-

* Corresponding author.
E-mail address: stweinman@eng.ua.edu (S.T. Weinman).

https://doi.org/10.1016/j.memlet.2023.100055
Received 27 May 2023; Received in revised form 28 June 2023; Accepted 28 June 2023

ent alkyl chain lengths in the IP reaction (Zhang et al., 2021). The NF membranes exhibited a more uniform pore size distribution and higher ion separation selectivity when the surfactants with longer alkyl chains were used (Zhang et al., 2021). Only a few studies have investigated the effect of surfactants on the synthesis of RO membranes (Park et al., 2022; Han et al., 2022; Kong et al., 2011; Duan et al., 2010; Gan et al., 2023; Jung et al., 2021). None of the RO membrane studies systematically varied the surfactant structure to examine the effect on the resultant membrane and its performance. For example, Park and coworkers used SDS and benzalkonium chloride to facilitate the diffusion of amines towards the organic phase by reducing the interfacial tension (IFT) between the organic and aqueous phases (Park et al., 2022), resulting in a denser polyamide layer having three time higher flux with 4% higher NaCl rejection compared to the control (Park et al., 2022). Kong et al. measured the MPD diffusion rate while using acetone as a co-solvent to control the reaction and adjust the membrane structure (Kong et al., 2011). In one study, the MPD diffusion rate in hexane with different concentrations of hexamethyl phosphoramide (HMPA) in solution was explored (Duan et al., 2010), whereas in another study, the effect of the surfactants on MPD diffusion and nanobubble formation was investigated (Gan et al., 2023). When using HMPA, the flux was improved by 73% and the NaCl rejection loss was < 0.2% compared to the control (Duan et al., 2010), while, using MPD and Tween-80 surfactant, the flux was increased by almost 20% (Gan et al., 2023). However, in all three of these instances, the MPD diffusion into the organic phase was measured at a free interface. These studies did not measure the MPD diffusion from support membranes to understand the direct diffusion kinetics which would be a more accurate depiction of the actual polyamide synthesis process (Duan et al., 2010; Gan et al., 2023). To understand MPD diffusion kinetics during IP, more direct experimental techniques must be used.

In this work, we investigated the structure-property relationship of seven surfactants on MPD diffusion towards the organic phase. We tested the hypothesis that negatively charged surfactants will lead to a higher MPD concentration in the organic phase due to favorable electrostatic interactions between MPD and the surfactant charged head group. We evaluated the critical micelle concentration (CMC) value of seven different surfactants and evaluated the MPD diffusion behavior across the aqueous/organic interface in the presence of these surfactants. Surfactants were anionic, cationic, and non-ionic in nature, with some having similar tail groups and different head groups, some having different lengths of alkyl chains, and some having different counterions. We believe this work will lead researchers to produce RO membranes with a more crosslinked polyamide layer with a higher rejection for the neutral charged molecules.

2. Materials and methods

2.1. Materials and chemicals

m-Phenylenediamine (MPD, 99%), sodium dodecyl sulfate (SDS, 98.5%), and sodium dodecylbenzenesulfonate (SDBS) were purchased from MilliporeSigma. Sodium laurate (SL, 98%) was purchased from Acros Organics. Hexadecyltrimethylammonium bromide (CTAB, >98%) and dodecyltrimethylammonium bromide (DTAB, >98%) were purchased from TCI America. Dodecyltrimethylammonium chloride (DTAC, 99%) was purchased from Beantown Chemical Corporation. Triton®X-100 (Electrophoresis reagent) was purchased from Alfa Aesar. The chemical structure of the surfactants used in this study is in Table S1 in the Supporting Information. Aqueous solutions were made with deionized water from a Millipore Synergy UV water purification system. Polysulfone PS20 membranes were used as received from Solecta, Inc. All membrane samples came from the center portion of the roll to avoid any possible edge defects.

Table 1
The chemical formulas of each surfactant and the interfacial tensions of each surfactant in *n*-Dodecane at 75% their critical micelle concentration. The error represents one standard deviation among at least three tests.

Surfactant	Chemical Formula	Interfacial Tension (mN/m)
SDS	$NaSO_4C_{12}H_{25}$	6.49 ± 0.21
SDBS	$NaSO_3C_{18}H_{29}$	6.13 ± 0.72
SL	$NaO_2C_{12}H_{23}$	9.77 ± 1.08
CTAB	$BrNC_{19}H_{42}$	7.18 ± 0.68
DTAB	$BrNC_{15}H_{34}$	8.48 ± 1.08
DTAC	$ClNC_{15}H_{34}$	13.69 ± 0.74
Triton®X-100	$C_{14}H_{22}O(C_2H_4O)_n$ (n = 9–10)	9.76 ± 0.13

2.2. Interfacial tension measurements

A DataPhysics Instruments OCA20 pendant drop tensiometer was used to measure the IFT for each sample at least three times. An injection needle (0.72 mm inner diameter) forms pendant droplets using a dispenser unit controlled by a PC. 2 μL droplets of aqueous surfactant solutions were used to measure the IFT in the fluid cell with *n*-dodecane. For each sample, disposable syringes and needles were used to avoid cross-contamination.

2.3. MPD diffusion tests

A PS20 membrane was soaked in DI water overnight. The wet membrane was placed on a Kimwipe with the non-woven fabric contacting the Kimwipe to dry the back of the membrane and then was placed on a glass plate with double-sided tape. The excess water present on the membrane surface was removed by shaking. The glass plate, membrane, and frame were held together using binder clips and is referred to as a frame setup. Next, 20 mL of aqueous MPD solution (2 w/v%) with or without surfactants was poured onto the membrane surface in the frame setup and left for 3.5 min. Then solution was poured off, the frame setup was disassembled, and a silicone seam roller from Home Depot was used to remove the aqueous MPD solution on the membrane surface in 1–2 passes. The surface of the membrane must be kept dry to avoid micro or macro-voids forming due to the presence of water droplets on the substrate surface. The frame setup was quickly reassembled and 20 mL of *n*-dodecane was poured on top of the MPD-soaked substrate and allowed to remain for a set time (15–60 s). Then, the *n*-dodecane solution was poured into a beaker and transferred to the collection vial for MPD concentration quantification. The amount of MPD concentration was measured using a HACH DR6000 UV–VIS Laboratory Spectrophotometer at 295 nm wavelength using plastic cuvettes (VWR). A calibration curve was constructed to calculate the MPD concentration (see Fig. S2 in the supporting information).

3. Results and discussion

3.1. Interfacial tension

Even though surfactants form adsorption layers at the water/organic solvent interface to reduce the system IFT, their adsorption abilities and behaviors differ with structure (Zhang et al., 2021). The arrangement and adsorption of surfactant molecules at water/oil interfaces pertain to their IFT (Zhang et al., 2021). We measured the IFT of the studied surfactants in *n*-dodecane to understand the effect of surfactants on interface adsorption. Table 1 provides the IFT of 75% CMC. The CMC of each surfactant was determined as described in section S2 of the supporting information. The change in the IFT of the system was mainly caused by the directional adsorption of surfactants at the aqueous solution/*n*-dodecane interface (Zhang et al., 2021). Among the anionic surfactants SDS and SDBS showed lower IFT compared to SL, which suggests the

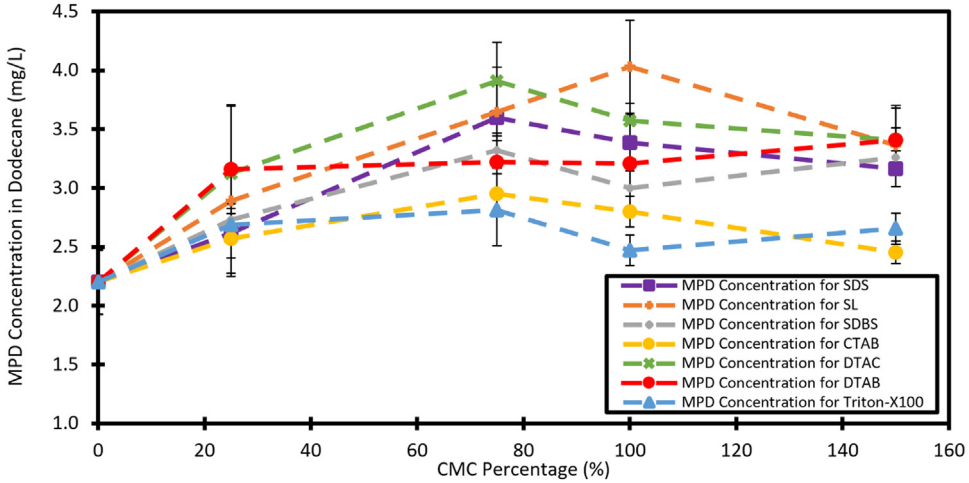

Fig. 1. MPD diffusion of different surfactants with 25, 75, 100 and 150% the CMC after 60 s of *n*-dodecane soaking. The error bars represent one standard deviation among at least three tests. The dashed lines between data points are included to aid in the visual comparison of the different surfactants and the varying concentrations.

head groups affects the arrangement and adsorption of the surfactant molecules at the interface. In case of cationic surfactants, CTAB showed lower IFT compared to DTAB and DTAC, which occurred due to the longer alkyl chain length of CTAB. These results were in agreement with a previous study, where the effect of different alkyl length on IFT was investigated (Zhang et al., 2021).

3.2. MPD diffusion

The MPD diffusion tests followed the same protocol as the IP process for fabricating polyamide RO membrane. During IP, the MPD and TMC react very quickly and make an initial incipient layer. Due to its weak partitioning from water to *n*-dodecane, MPD diffusing into *n*-dodecane is the rate-limiting step as compared with its reaction with TMC in *n*-dodecane. This incipient polyamide layer limits the MPD diffusion across the interface. In our MPD diffusion test, instead of TMC being present in the *n*-dodecane solution, only *n*-dodecane was used to determine the effect of surfactants on MPD diffusion into the organic phase without any reaction. As a result, the maximum MPD diffusion towards the interface happens.

3.2.1. MPD diffusion at a fixed time

The MPD diffusion was measured by using surfactants at different concentrations at a fixed time (60 s). All the surfactants were used at 25, 75, 100, and 150% the surfactant CMC and Fig. 1 shows that the surfactants exhibited significantly higher concentration compared to the control with no surfactant (0% CMC). Most of the surfactants showed the highest MPD concentration at 75% CMC except for SL which exhibited a maximum MPD concentration at 100% CMC. For all the surfactants, the MPD concentration at 100% CMC was similar to 150% CMC. This is due to the surfactants forming micelles at and above the CMC concentration. These micelles were not involved in facilitating the MPD diffusion but obstructed the water passage of the membrane and restricted MPD from diffusing towards the water/*n*-dodecane interface (Aryanti et al., 2020; Madaeni and Samieirad, 2010). The micelle size may impact the small differences between 100 and 150% CMC as a previous study compared the micelle size of five different surfactants, including SDS, CTAB, and DTAB, and found that DTAB had the smallest micelle radius of the five surfactants (Santos et al., 2016). It is possible that the DTAB micelles were small enough to not obstruct the support membrane pores as significantly as the other surfactants. While the dashed lines may go up for some surfactants and may go down for others, the error bars for the surfactants overlap at 100% and 150% CMC, so it is challenging to justify that the average values are significantly different from one another. Interestingly, DTAC at 25 and 75% the CMC (and DTAB at 25% the CMC) have higher amounts of MPD diffusion than the other surfactants. This will be discussed further below with Fig. 2.

3.2.2. MPD diffusion at a fixed surfactant concentration

MPD diffusion was tested using 0% and 75% CMC for each surfactant for different *n*-dodecane soaking times (Fig. 2). For all cases, there was an increase in MPD concentration in *n*-dodecane with the increase in soaking time. Among all the surfactants, Triton®X-100 showed the lowest MPD concentration in the diffusion test. As Triton®X-100 was not ionic in nature, it did not contribute much interaction with MPD because there were no charged moieties present to interact with the slightly positively charged MPD. Compared to the control, the addition of anionic surfactants SDS, SDBS, and SL increased the MPD diffusion at 25, 40 and 60 s. A negatively charged sulfonic group on SDS and SDBS and a negatively charged carboxylic group on SL attracts the slightly positively charged MPD molecule at the water/*n*-dodecane interface, which increases the accumulation of MPD monomers and enhances the MPD diffusion in a qualitatively similar manner at lower soaking times. Since the benzene rings restrict the interfacial packing density, SDBS increases the MPD diffusion less effectively than SDS at longer soaking times due to steric hindrance.

In the case of cationic surfactants, we expected to see a lower MPD concentration than the anionic surfactants due to the electrostatic repulsion between the positively charged head group of surfactants and positively charged MPD (Zhang et al., 2023; Jia et al., 2014). Surprisingly, the MPD diffusion of DTAB and DTAC was comparable to that of anionic surfactants. We believe, MPD may have interacted with the cationic quaternary ammonium head groups of DTAB and DTAC via cation-pi interaction, which could have accelerated MPD diffusion. The cation-pi interaction between positively charged metal ions and MPD pi-cloud was observed previously (Pandian et al., 2015). The MPD concentration using DTAC was higher than using DTAB. The higher electronegativity and smaller size of Cl^- ions compared to Br^- ions attracted more MPD molecules and accelerated the MPD diffusion via electrostatic interactions (Fouda et al., 2012).

Among the cationic surfactants, CTAB showed comparatively lower MPD diffusion compared to DTAC and DTAB. Because of the higher hydrophobic interactions between CTAB's long alkyl chains and lower IFT in *n*-dodecane compared to DTAB and DTAC, the surfactant molecules at the interface were assumed to have a higher degree of order and orientation. This is in agreement with a previous study where the IFT of anionic surfactants with different alkyl tail lengths was measured and they showed the decrease in the IFT was caused by the directional adsorp-

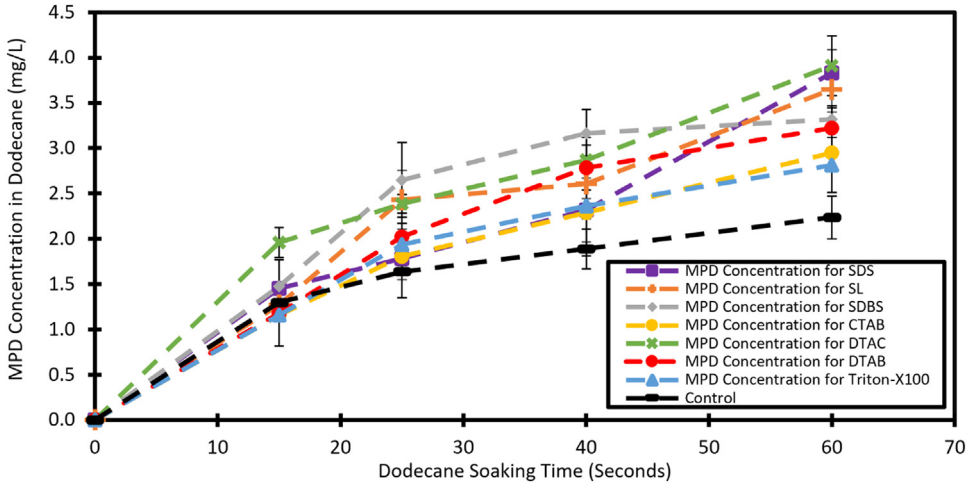

Fig. 2. MPD diffusion of different surfactants with 75% CMC after 15, 25, 40 and 60 s of *n*-dodecane soaking. The error bars represent one standard deviation among at least three tests. The dashed lines between data points are included to aid in the visual comparison of the different surfactants and the varying concentrations.

tion of surfactants at the water/*n*-hexane interface (Zhang et al., 2021). The formation of a tightly packed monolayer of CTAB molecules caused steric hindrance and slowed down the diffusion of MPD molecules toward the interface.

4. Conclusion

Surfactants play an important role in the interfacial diffusion of diamine monomers into the organic phase, affecting the overall IP process to form polyamide RO membranes. A more complete polyamide active layer can be formed when the diamine monomers are properly fluxed across the interface between water and *n*-dodecane in a dynamic network. Unexpectedly, our testable hypothesis was not fully supported by the results. Most surfactants behaved as expected, with anionic ones providing the highest amount of MPD diffusion into the organic phase. However, DTAC (and to some extent DTAB), did not obey this trend. Future studies will investigate (1) more detailed surfactant properties, (2) a more comprehensive list of surfactants, especially to probe the effect of the counterion, (3) dominant interactions responsible for MPD diffusion by using other molecules with different chemical structures than MPD in the same system, and (4) whether the surfactants are present in the polyamide layer after synthesis (unlikely unless the surfactant concentration used in the synthesis was above the CMC value (Liang et al., 2020)).

This surfactant-assisted IP can easily be implemented for the scalable fabrication of ultra-selective RO membranes for small, neutral molecule separation since it requires little modification of established TFC-PA RO membrane fabrication techniques. Future studies will focus on correlating these MPD diffusion results with polyamide layer structure properties and RO membrane performance properties.

Statement of novelty

This contribution reports on systematically varying the surfactant structure to determine the amount of m-phenylenediamine (MPD) that transports across the aqueous/organic interface. We studied seven surfactants at varying concentrations and contact times to determine the effects of surfactant properties on MPD crossover directly from a membrane support. Previous literature focuses mostly on nanofiltration membranes using piperazine but few studies have investigated the surfactant effect on MPD-based reverse osmosis (RO) membranes. The immediacy for publication is to showcase that surfactant structure does play a role in MPD transport and requires further investigation into how the surfactants influence RO membrane formation.

Funding information

S.H. was supported by an Alabama EPSCoR Graduate Research Scholars Program Fellowship. The authors would like to acknowledge the financial support of the National Science Foundation (NSF) under award number OIA-1928812. Any opinions, findings, conclusions, and/or recommendations expressed in this material are those of the author(s) and do not necessarily reflect the views of the NSF.

Declaration of Competing Interest

The authors declare no conflict of interest.

CRediT authorship contribution statement

Shahriar Habib: Conceptualization, Data curation, Formal analysis, Investigation, Methodology, Validation, Visualization, Writing – original draft, Writing – review & editing. **Bryn E. Larson:** Data curation, Formal analysis, Investigation, Methodology, Validation, Visualization. **Steven T. Weinman:** Conceptualization, Formal analysis, Funding acquisition, Methodology, Project administration, Supervision, Validation, Visualization, Writing – review & editing.

Data availability

Data will be made available on request.

Acknowledgments

S.H. was supported by an Alabama EPSCoR Graduate Research Scholars Program Fellowship. The authors would like to acknowledge the financial support of the National Science Foundation (NSF) under award number OIA-1928812. Any opinions, findings, conclusions, and/or recommendations expressed in this material are those of the author(s) and do not necessarily reflect the views of the NSF. The authors thank Solecta, Inc. for kindly provided the membranes used in this study. We thank Dr. Amanda Koh for the use of her pendant drop tensiometer.

Supplementary materials

Supplementary material associated with this article can be found, in the online version, at doi:10.1016/j.memlet.2023.100055.

References

Ang, M.B.M.Y., Tang, C.L., De Guzman, M.R., Maganto, H.L.C., Caparanga, A.R., Huang, S.H., Tsai, H.A., Hu, C.C., Lee, K.R., Lai, J.Y., 2020. Improved performance of thin-film nanofiltration membranes fabricated with the intervention of surfactants having different structures for water treatment. Desalination 481, 114352. doi:10.1016/j.desal.2020.114352.

Aryanti, N., Nafiunisa, A., Kusworo, T.D., Wardhani, D.H., 2020. Micellar-enhanced ultrafiltration using a plant-derived surfactant for dye separation in wastewater treatment. Membranes 10 (9), 220.

Bai, J., Lai, W., Gong, L., Xiao, L., Wang, G., Shan, L., Luo, S., 2022. Ionic liquid regulated interfacial polymerization process to improve acid-resistant nanofiltration membrane permeance. J. Membr. Sci. 641, 119882. doi:10.1016/j.memsci.2021.119882.

Duan, M., Wang, Z., Xu, J., Wang, J., Wang, S., 2010. Influence of hexamethyl phosphoramide on polyamide composite reverse osmosis membrane performance. Sep. Purif. Technol. 75 (2), 145–155. doi:10.1016/j.seppur.2010.08.004.

Fang, W., Shi, L., Wang, R., 2013. Interfacially polymerized composite nanofiltration hollow fiber membranes for low-pressure water softening. J. Membr. Sci. 430, 129–139. doi:10.1016/j.memsci.2012.12.011.

Farahbakhsh, J., Vatanpour, V., Khoshnam, M., Zargar, M., 2021. Recent advancements in the application of new monomers and membrane modification techniques for the fabrication of thin film composite membranes: a review. React. Funct. Polym. 166, 105015. doi:10.1016/j.reactfunctpolym.2021.105015.

Fouda, A., Elewady, Y., Abd El-Aziz, H., Ahmed, A., 2012. Corrosion inhibition of carbon steel in 0.5M HCl solution using cationic surfactants. Int. J. Electrochem. Sci 7 (10), 456–510.

Gan, Q., Peng, L.E., Yang, Z., Sun, P.F., Wang, L., Guo, H., Tang, C.Y., 2023. Demystifying the role of surfactant in tailoring polyamide morphology for enhanced reverse osmosis performance: mechanistic insights and environmental implications. Environ. Sci. Technol. 57 (4), 1819–1827. doi:10.1021/acs.est.2c08076.

Grzebyk, K., Armstrong, M.D., Coronell, O., 2022. Accessing greater thickness and new morphology features in polyamide active layers of thin-film composite membranes by reducing restrictions in amine monomer supply. J. Membr. Sci. 644, 120112. doi:10.1016/j.memsci.2021.120112.

Habib, S., Weinman, S.T., 2021. A review on the synthesis of fully aromatic polyamide reverse osmosis membranes. Desalination 502, 114939. doi:10.1016/j.desal.2021.114939.

Habib, S., Weinman, S.T., 2022. Modification of polyamide reverse osmosis membranes for the separation of urea. J. Membr. Sci. 655, 120584. doi:10.1016/j.memsci.2022.120584.

Han, X., Wang, Z., Wang, J., 2022. Preparation of highly selective reverse osmosis membranes by introducing a nonionic surfactant in the organic phase. J. Membr. Sci. 651, 120453. doi:10.1016/j.memsci.2022.120453.

Hu, A., Liu, Y., Zheng, J., Wang, X., Xia, S., Van der Bruggen, B., 2023. Tailoring properties and performance of thin-film composite membranes by salt additives for water treatment: a critical review. Water Res. 234, 119821. doi:10.1016/j.watres.2023.119821.

Jia, Q., Han, H., Wang, L., Liu, B., Yang, H., Shen, J., 2014. Effects of CTAC micelles on the molecular structures and separation performance of thin-film composite (TFC) membranes in forward osmosis processes. Desalination 340, 30–41. doi:10.1016/j.desal.2014.02.017.

Jiang, C., Tian, L., Zhai, Z., Shen, Y., Dong, W., He, M., Hou, Y., Niu, Q.J., 2019. Thin-film composite membranes with aqueous template-induced surface nanostructures for enhanced nanofiltration. J. Membr. Sci. 589, 117244. doi:10.1016/j.memsci.2019.117244.

Jung, K.H., Kim, H.J., Kim, M.H., Seo, H., Lee, J.C., 2021. Superamphiphilic zwitterionic block copolymer surfactant-assisted fabrication of polyamide thin-film composite membrane with highly enhanced desalination performance. J. Membr. Sci. 618, 118677. doi:10.1016/j.memsci.2020.118677.

Kong, C., Shintani, T., Kamada, T., Freger, V., Tsuru, T., 2011. Co-solvent-mediated synthesis of thin polyamide membranes. J. Membr. Sci. 384 (1), 10–16. doi:10.1016/j.memsci.2011.08.055.

Li, Y., Wang, S., Li, H., Kang, G., Sun, Y., Yu, H., Jin, Y., Cao, Y., 2022. Preparation of highly selective nanofiltration membranes by moderately increasing pore size and optimizing microstructure of polyamide layer. J. Membr. Sci. 643, 120056. doi:10.1016/j.memsci.2021.120056.

Liang, Y., Zhu, Y., Liu, C., Lee, K.R., Hung, W.S., Wang, Z., Li, Y., Elimelech, M., Jin, J., Lin, S., 2020a. Polyamide nanofiltration membrane with highly uniform sub-nanometre pores for sub-1 A precision separation. Nat. Commun. 11 (1), 2015. doi:10.1038/s41467-020-15771-2.

Liang, Y., Zhu, Y., Liu, C., Lee, K.R., Hung, W.S., Wang, Z., Li, Y., Elimelech, M., Jin, J., Lin, S., 2020b. Polyamide nanofiltration membrane with highly uniform sub-nanometre pores for sub-1 Å precision separation. Nat. Commun. 11 (1), 2015. doi:10.1038/s41467-020-15771-2.

Liu, C., Wang, C., Guo, Y., Zhang, J., Cao, Y., Liu, H., Hu, Z., Zhang, C., 2019. High-performance polyamide membrane with tailored water channel prepared via bionic neural networks for textile wastewater treatment. J. Mater. Chem. A 7 (12), 6695–6707. doi:10.1039/C9TA00031C.

Liu, Y., Yan, W., Wang, Z., Wang, H., Zhao, S., Wang, J., Zhang, P., Cao, X., 2020. 1-methylimidazole as a novel additive for reverse osmosis membrane with high flux-rejection combinations and good stability. J. Membr. Sci. 599, 117830. doi:10.1016/j.memsci.2020.117830.

Lu, X., Elimelech, M., 2021. Fabrication of desalination membranes by interfacial polymerization: history, current efforts, and future directions. Chem. Soc. Rev. 50 (11), 6290–6307. doi:10.1039/D0CS00502A.

Madaeni, S.S., Samieirad, S., 2010. Chemical cleaning of reverse osmosis membrane fouled by wastewater. Desalination 257 (1), 80–86. doi:10.1016/j.desal.2010.03.002.

Pandian, S., Katha, A.R., Moon, J.H., Kolake, S.M., Han, S., 2015. Exploring the effect of additives on polyamide membrane surface for seawater desalination using density functional tools. Desalination 367, 28–36. doi:10.1016/j.desal.2015.03.034.

Park, S.J., Lee, M.S., Choi, W., Lee, J.H., 2022. Biocidal surfactant-assisted fabrication of thin film composite membranes with excellent and durable anti-biofouling performance. Chem. Eng. J. 431, 134114. doi:10.1016/j.cej.2021.134114.

Santos, M., Tavares, F., Biscaia, E., 2016. Molecular thermodynamics of micellization: micelle size distributions and geometry transitions. Braz. J. Chem. Eng. 33, 515–523.

Sarkar, P., Modak, S., Karan, S., 2021. Ultraselective and highly permeable polyamide nanofilms for ionic and molecular nanofiltration. Adv. Funct. Mater. 31 (3), 2007054. doi:10.1002/adfm.202007054.

Wittbecker, E.L., Morgan, P.W., 1959. Interfacial polycondensation. I. J. Polym. Sci. 40 (137), 289–297.

Xiang, J., Xie, Z., Hoang, M., Zhang, K., 2013. Effect of amine salt surfactants on the performance of thin film composite poly(piperazine-amide) nanofiltration membranes. Desalination 315, 156–163. doi:10.1016/j.desal.2012.10.038.

Xiang, J., Xie, Z., Hoang, M., Ng, D., Zhang, K., 2014. Effect of ammonium salts on the properties of poly(piperazineamide) thin film composite nanofiltration membrane. J. Membr. Sci. 465, 34–40. doi:10.1016/j.memsci.2014.03.074.

Zhang, Z., Kang, G., Yu, H., Jin, Y., Cao, Y., 2019. From reverse osmosis to nanofiltration: precise control of the pore size and charge of polyamide membranes via interfacial polymerization. Desalination 466, 16–23. doi:10.1016/j.desal.2019.05.001.

Zhang, F., Fan, J.b., Wang, S., 2020. Interfacial polymerization: from chemistry to functional materials. Angew. Chem. Int. Ed. 59 (49), 21840–21856.

Zhang, R., Zhu, Y., Zhang, L., Lu, Y., Yang, Z., Zhang, Y., Jin, J., 2021. Polyamide nanofiltration membranes from surfactant-assembly regulated interfacial polymerization: the effect of alkyl chain. Macromol. Chem. Phys. 222 (20), 2100222. doi:10.1002/macp.202100222.

Zhang, X., Cui, H.M., Gao, Y., Yan, Z.W., Yan, X., Chen, Y., Guo, X.J., Lang, W.Z., 2023. Surfactant-induced intervention in interfacial polymerization to develop highly-selective thin-film composite membrane for forward osmosis process. Desalination 558, 116617. doi:10.1016/j.desal.2023.116617.

Supporting Information

Effect of Surfactant Structure on Diamine Diffusion for Interfacial Polymerization

Shahriar Habib, Bryn E, Larson and Steven T. Weinman*

Department of Chemical and Biological Engineering, The University of Alabama, Tuscaloosa, AL 35487, USA

*Corresponding author: Tel: +1 (205)-348-8516, Fax: +1 (205)-348-7558. Email address: stweinman@eng.ua.edu

S1. Surfactant Chemical Structures

The chemical structure of each surfactant used in this study is presented in **Table S1**.

Table S1. The chemical structure of the surfactants used in this study.

Surfactant	Chemical Structure
SDS	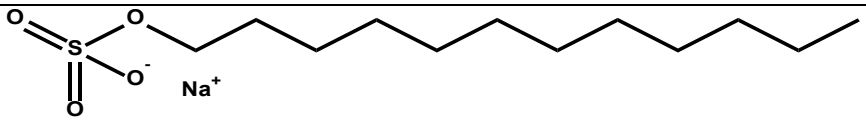
SDBS	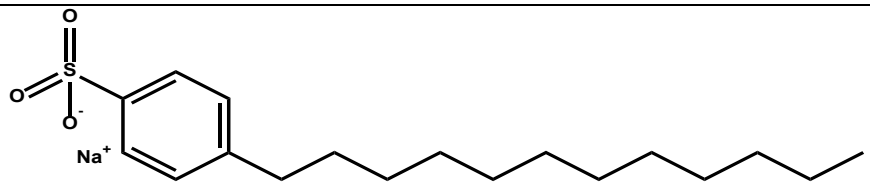
SL	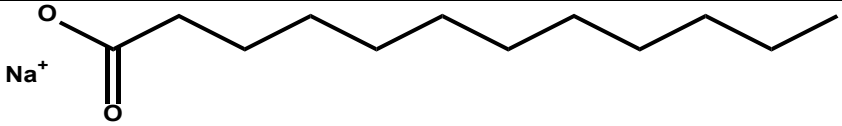
CTAB	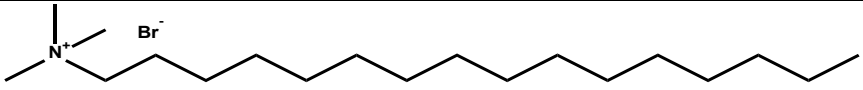
DTAB	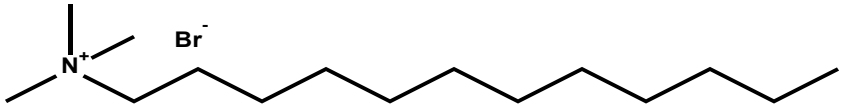
DTAC	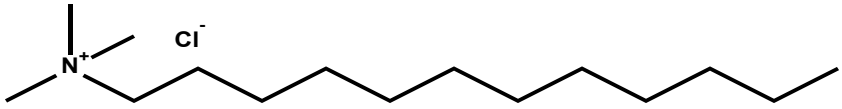
Triton®X-100	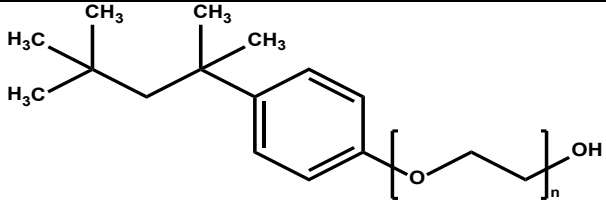

S2. Determining the CMC of different surfactants

S2.1. Conductivity Measurements Methods

For each surfactant, solutions were made at varying surfactant concentrations in DI water. The conductivity of the solution was measured using a VWR Traceable Bench/Portable Conductivity Meter. The CMC value of the surfactants was determined from the concentration-conductivity plot. Where there is a change in slope, that is the CMC. This test could not be done with Triton®X-100 because it is a non-ionic surfactant and does not exhibit any conductivity in solution. This data is presented in **Figures S1A-F**.

S2.2. Surface Tension Measurements

An OCA20 pendant drop tensiometer (DataPhysics Instruments, Charlotte, NC, USA) was used to measure surface tension for Triton®X-100 samples at least three times to get an average value with standard deviation. An injection needle (0.72 mm in inside diameter) forms pendant droplets using a dispenser unit controlled by a PC. Droplets of dilute surfactant solutions were 2 µL in volume in the experiments. The surface tension was measured in the air. For each sample, disposable syringes and needles were used to avoid cross-contamination. This data is presented in **Figure S1G**.

S2.3. CMC Evaluation

The CMC value of each surfactant was determined using conductivity and surface tension measurements. The CMC value of the surfactant was similar to the values reported in the literature (see **Table S2**) [1-7]. Except for the Triton®X-100 and CTAB, all of the surfactants have the same alkyl chain length. SDBS has a similar alkyl chain length but with a benzyl group between the sulfonate head group and the alkyl chain. The CMC value of the anionic and cationic surfactants with the same alkyl tails was dependent on the chemical structure of the head group. At the CMC, molecules of surfactants aggregate to form micellar macroions [8]. Since micellar macroions have a lower mobility, they contribute less to the overall conductivity of the solution [8]. Conductivity vs. surfactant concentration shows a detectable slope change at a particular point, which can be identified as the CMC.

Table S2. CMC of surfactants

Surfactant	CMC Value (mM)	Literature Value (mM)
SDS	8.00	8.00 - 8.20 [1, 2, 7]
SDBS	2.30	2.30 - 2.73 [3, 6]
SL	30.00	24.00 - 30.00 [2, 4]
CTAB	0.92	0.80 - 0.92 [1, 2]
DTAB	15.00	14.90 - 60.00 [2, 5]
DTAC	20.00	15.00 - 20.30 [2, 5]
Triton®X-100	0.34	0.24 – 0.27 [2, 7]

In our experiments, we found a considerable difference between the CMC of SDBS and SDS. Surfactants with a more hydrophobic character (such as the benzyl ring of SDBS) tend to have a lower CMC in aqueous medium. [9]. A higher CMC was observed for SL than for SDS. In a previous study, the log binding constants (log K_B) between polycyclic aromatic hydrocarbons and surfactants were investigated [10]. The log K_B is an indication of the hydrophobic interactions between a surfactant and an organic compound, where a larger number indicates more interactions [10]. The log K_B of the polycyclic aromatic hydrocarbons with SDS in that study was found to be higher than the SL. As a result, SDS had a lower CMC value than SL due to its higher hydrophobicity.

The CMC of cationic surfactants also was determined. The CMC of DTAB was higher than SDS. This might be due to SDS's higher hydrophobicity compared to DTAB, in agreement with an earlier study showing SDS had a higher affinity for AgNPs than DTAB because of its higher hydrophobicity [11]. When comparing the CMC values of DTAB and CTAB, where CTAB had a longer alkyl tail but the same head groups as DTAB, and the CMC decreased greatly as the alkyl tail length was increased from DTAB to CTAB [12]. When the CMC values of DTAC and DTAB were compared, the counter ion effect becomes apparent, which is in agreement with literature [13]. A reduction in CMC is observed when the counter ion is changed from Cl^- to Br^-. Because the counter ion's size increases from 0.181 nm (Cl^-) to 0.196 nm (Br^-), it becomes less hydrated [14]. Micellar surfaces are more readily able to absorb weakly hydrated ions (Br^-) because the charge repulsion between the polar groups is decreased [14]. On the other hand, polar water molecules partially screen the charge on heavily hydrated ions (Cl^-). Because of this, Cl^- counterions have less effect on charge repulsion between the head groups [14]. Since Triton®X-

100 is a non-ionic surfactant, the CMC value could not be determined using conductivity measurements. The CMC of the Triton®X-100 was evaluated via surface tension measurement. The CMC of the Triton®X-100 was found to be significantly lower than both anionic and cationic surfactants. The presence of the benzene ring and multiple methyl groups increased the hydrophobicity of the molecules, which in turn reduced the CMC value significantly.

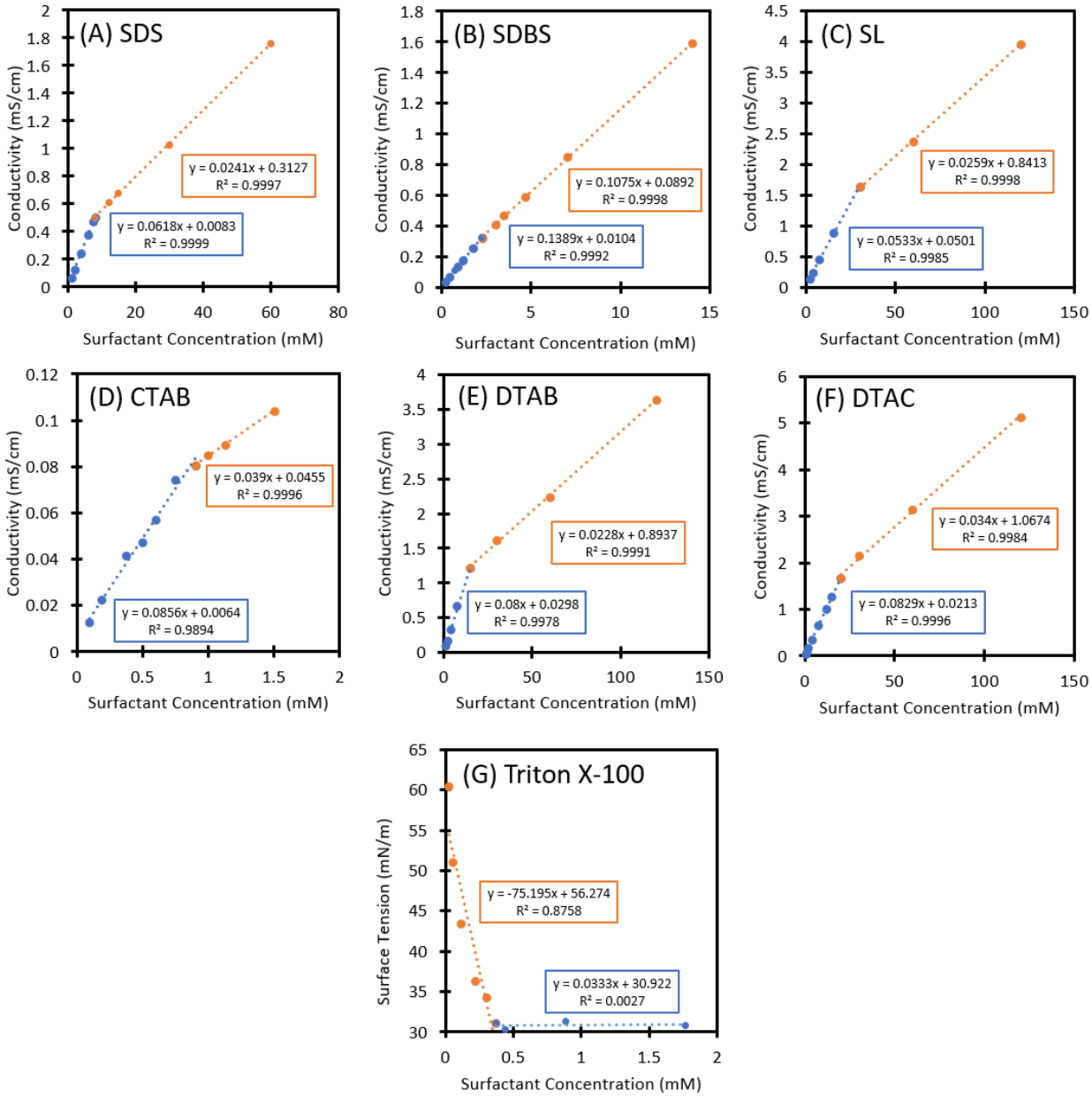

Figure S1. Conductivity test for determining the CMC of (A) SDS, (B) SDBS, (C) SL, (D) CTAB, (E) DTAB, (F) DTAC and surface tension measurement for determining the CMC of (G) Triton®X-100.

S2. Calibration curve for MPD in *n*-dodecane

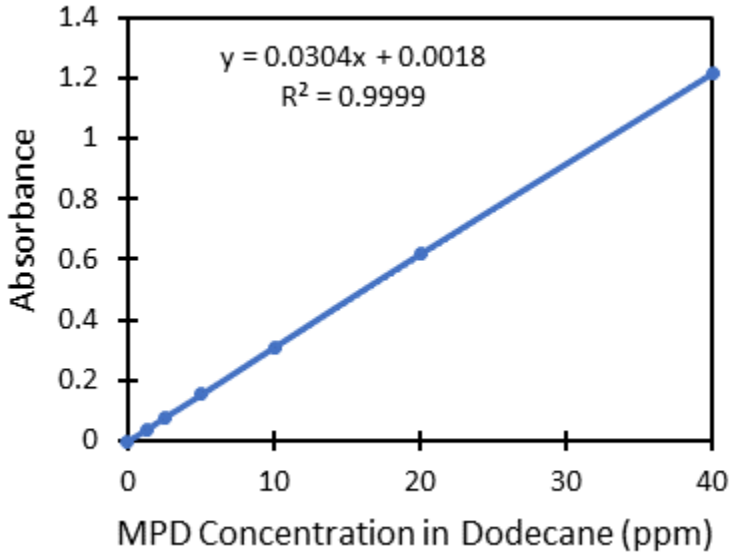

Figure S2. Calibration curve for MPD in *n*-dodecane.

References

[1] Z. Ahmad, M. Siddiq, A. Muhammad Khan, A. Shah, Fluorescence Investigations of the Association of PEO-PBO-PEO Triblock Copolymers in the Presence of Ionic Surfactants SDS and CTAB, Advances in Research, 2 (2014) 70-79.

[2] K. Kalyanasundaram, J.K. Thomas, Environmental effects on vibronic band intensities in pyrene monomer fluorescence and their application in studies of micellar systems, Journal of the American Chemical Society, 99 (1977) 2039-2044.

[3] H. Om, G.A. Baker, K. Behera, V. Kumar, K.K. Verma, S. Pandey, Self-Probing of Micellization within Phenyl-Containing Surfactant Solutions, ChemPhysChem, 11 (2010) 2510-2513.

[4] F.E. Stanley, A.M. Warner, E. Schneiderman, A.M. Stalcup, Rapid determination of surfactant critical micelle concentrations using pressure-driven flow with capillary electrophoresis instrumentation, Journal of Chromatography A, 1216 (2009) 8431-8434.

[5] B.L. Bales, R. Zana, Characterization of Micelles of Quaternary Ammonium Surfactants as Reaction Media I: Dodeclytrimethylammonium Bromide and Chloride, The Journal of Physical Chemistry B, 106 (2002) 1926-1939.

[6] A.K. Sood, M. Aggarwal, Evaluation of micellar properties of sodium dodecylbenzene sulphonate in the presence of some salts, Journal of Chemical Sciences, 130 (2018) 1-7.
[7] V. Singh, R. Tyagi, Investigations of mixed surfactant systems of lauryl alcohol-based bissulfosuccinate anionic gemini surfactants with conventional surfactants: A fluorometric study, Journal of Taibah University for Science, 9 (2015) 477-489.
[8] P. Di Profio, S. Arca, R. Germani, G. Savelli, Surfactant promoting effects on clathrate hydrate formation: Are micelles really involved?, Chemical Engineering Science, 60 (2005) 4141-4145.
[9] N. Salahudeen, A.A. Rasheed, Kinetics and thermodynamics of hydrolysis of crystal violet at ambient and below ambient temperatures, Scientific Reports, 10 (2020) 21929.
[10] A.K. Sarker, R.S. Brown, Determining binding of polycyclic aromatic hydrocarbons to micelles formed by SDS and SOL using semi-equilibrium dialysis, Ecotoxicology and Environmental Safety, 208 (2021) 111635.
[11] O. Naderi, M. Nyman, M. Amiri, R. Sadeghi, Synthesis and characterization of silver nanoparticles in aqueous solutions of surface active imidazolium-based ionic liquids and traditional surfactants SDS and DTAB, Journal of Molecular Liquids, 273 (2019) 645-652.
[12] A. Ali, S. Uzair, N.A. Malik, M. Ali, Study of interaction between cationic surfactants and cresol red dye by electrical conductivity and spectroscopy methods, Journal of Molecular Liquids, 196 (2014) 395-403.
[13] M.T. Bashford, E.M. Woolley, Enthalpies of dilution of aqueous decyl-, dodecyl-, tetradecyl-, and hexadecyltrimethylammonium bromides at 10, 25, 40, and 55.degree.C, The Journal of Physical Chemistry, 89 (1985) 3173-3179.
[14] S.K. Mehta, K.K. Bhasin, R. Chauhan, S. Dham, Effect of temperature on critical micelle concentration and thermodynamic behavior of dodecyldimethylethylammonium bromide and dodecyltrimethylammonium chloride in aqueous media, Colloids and Surfaces A: Physicochemical and Engineering Aspects, 255 (2005) 153-157.